Proceedings of the 9th U.S. National and 10th Canadian Conference on Earthquake Engineering
Compte Rendu de la 9ième Conférence Nationale Américaine et
10ième Conférence Canadienne de Génie Parasismique
July 25-29, 2010, Toronto, Ontario, Canada • Paper No 275

# UNDERPINNING OF RAFT SLAB FOUNDATION FOR SEISMIC REMEDIATION USING JET GROUTING AND ITS QA METHODS

W. B. Gohl[1] and P. Zabeti[2]

## ABSTRACT

A seismic upgrade of an existing raft slab foundation to support a future electrical transformer owned by B.C Hydro and the QA methods of its construction are described. The raft slab was underpinned using jet grout columns, each having a nominal diameter of 1m, and were extended through liquefiable soils to limit post-seismic displacements of the slab and improve bearing capacity. The soil-structure interaction analysis of the JG columns is described as well as methods of construction and quality control.

## Introduction

In 2008 a geotechnical investigation and a series of design analyses were carried out to evaluate foundation vulnerabilities for an existing raft slab foundation under design levels of earthquake shaking. The raft slab is located within the Walters Electrical Substation in North Vancouver, B.C. and is owned by British Columbia Hydro & Power Authority (BC Hydro). At the time of the geotechnical investigation, no structures existed on the slab and BC Hydro proposed placing a new electrical transformer on it. The initial geotechnical assessment indicated a high seismic liquefaction potential of the near surface sand and gravel subsoils, resulting in the potential for significant seismic displacements of the raft slab and transformer. Different methods of improvement of the foundation soils were evaluated and ultimately a decision was made to use jet grout (JG) columns to underpin the raft slab. The intent of the JG columns was to reduce seismically induced movements of the slab. A series of analyses were subsequently carried out to examine the soil-column-raft slab interaction during seismic shaking. Methods of construction and quality control employed during construction are also described.

## Geotechnical Background

The existing raft slab has a plan dimension of about 7.8m x 7.5m and a slab thickness of about 1m. The base of the slab below existing ground surface is approximately 0.9m. Becker drilling and Becker Density Testing (BDT), including hammer energy measurements during the BDT using pile driving analyzer equipment, were carried out adjacent to the raft slab.

The soils investigation indicated the following soil profile relative to the existing ground surface:

0 – 4 m depth: Compact to dense, sandy gravel and cobbles (FILL)
4 – 8 m depth: Very loose to loose, sand and gravel with shell fragments
8 – 10.4 m depth: Compact, sand and gravel with shell fragments

[1] Principal Geotechnical Engineer, MEG Consulting Ltd., Richmond, British Columbia, Canada
[2] Geotechnical Engineer, BC Hydro, Burnaby, British Columbia, Canada

10.4 – 13.4 m depth: Compact, sand and gravel with cobbles grading to sand, some silt
13.4 – 18.3 m depth: Compact to dense, sand with gravel and cobbles

Piezometer measurements over time indicated a minimum depth to groundwater of 4 m.

The BDT energy measurements are summarized in Figure 1, which plots average energy efficiency (e) per blow for each 0.3 m of casing penetration relative to the maximum standard energy of 11 kJoules. The data indicates typical air hammer efficiencies of 25 to 30% down to 18.3 m depth. Measured uncorrected Becker blow counts ($N_b$) per 0.3m of casing penetration and corrected $N_{b,30} = N_b\, e(\%)/30\%$ are also presented in Figure 1.

The correlation between $N_{b,30}$ and Standard Penetration Test $N_{60}$ value is complicated by values of casing friction acting on the Becker casing (Sy, 1997). Sy has proposed charts relating $N_{b,30}$ and $N_{60}$ as a function of casing friction which was not measured directly during the present testing. We have estimated casing friction using empirically-based procedures suggested by Sy for predominantly sand or gravel sites and then used the Sy charts to estimate $N_{60}$. Given the uncertainty in casing friction measurements, we have also used correlations between $N_{b,30}$ and $N_{60}$ at other sites in North Vancouver in similar sand and gravel deposits as exist at the Walters Substation and using identical Becker casing diameters for the various sites. The latter data indicated a reasonable trend in the data was given as $N_{b,30} \approx N_{60}$ for depths of penetration less than about 15m.

Plots of inferred $N_{60}$ versus depth based on the Sy (1997) method (Method A) and using the average $N_{b,30} \approx N_{60}$ trend line from other sites (Method B) are shown in Figure 2. The two methods agree closely for lower Becker penetration resistances while the Sy method gives higher $N_{60}$ values for higher penetration resistances. We have adopted Method B in selecting a design value of $N_{60}$ versus depth. Stress normalized $N_{1,60}$ values were then computed as $N_{1,60} = C_n\, N_{60}$ where $C_n$ is a stress level correction factor given as $[\sigma'_{vo} / p_{atm}]^{0.5}$ . Here $\sigma'_{vo}$ is the vertical effective pressure at a depth under consideration and $p_{atm}$ is the atmospheric pressure (= 101.3 kPa). $C_n$ is assigned a maximum value of 1.7 at shallow depths. A plot of inferred $N_{1,60}$ versus depth is shown in Figure 2 which has been used for purposes of seismic liquefaction evaluation at the site. The low inferred $N_{1,60}$ values less than 10 between the 4 and 8m depth suggest a high seismic liquefaction potential.

## Seismic Site Response Analysis and Liquefaction Assessment

Seismic input motions representative of the 2475 year return period earthquake have been considered for the site, consistent with the seismic design provisions of the 2005 National Building Code of Canada (NBCC). A series of 10 earthquake input motions, representative of outcrop motions occurring on Site Class C soils (dense soils or soft rock having shear wave velocities in the range of 360 to 750 m/sec) were used in site response analysis. Each seismic input motion was filtered to match a target elastic response spectrum (5% damping case) specified by the NBCC for the North Vancouver area. The filtered motions had a peak acceleration of 0.45 g.

Following selection of the input earthquake motions, these were assumed to propagate vertically

as horizontal shear waves. The computer program DESRA-2C (Lee and Finn, 1978) was used for this analysis. The input motions were applied at the 80m depth where available geotechnical information in the surrounding area indicated very dense sand and gravel deposits with shear wave velocities in excess of 400 m/sec were present. An energy absorbing bottom boundary was used in the model which resulted in reduced wave energy being propagated vertically.
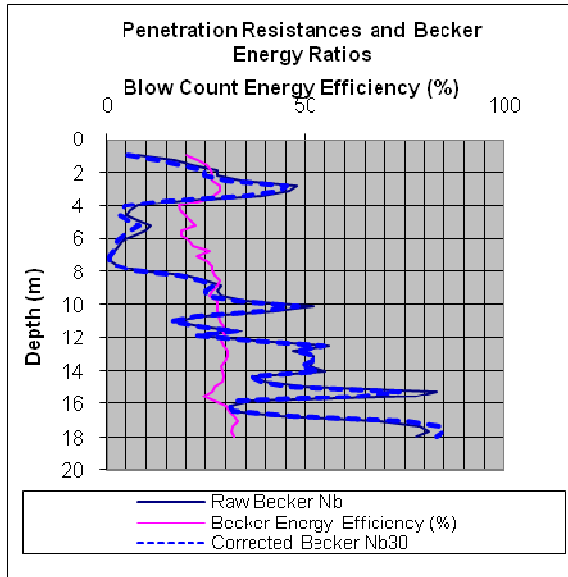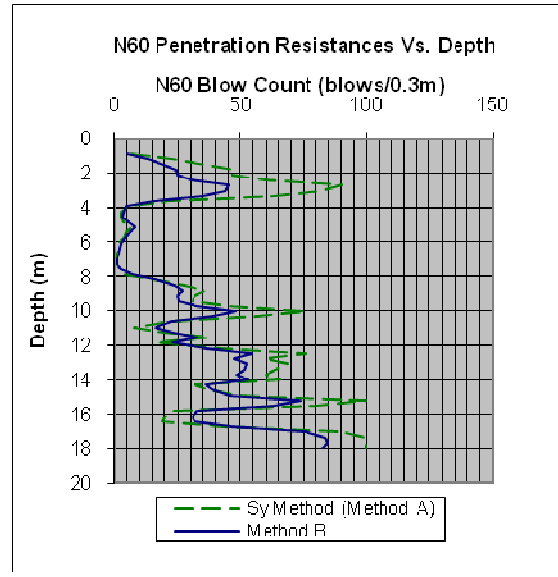


Figure 1: Becker penetration test data.



Figure 2: Inferred $N_{60}$ versus depth based on Sy (1997) method and correlations between $N_{60}$ and $N_{b30}$ established from available data in North Vancouver, B.C.

DESRA-2C is a non-linear analysis and considers the cyclic hysteretic response of each soil layer. It requires as input the shear strength on the horizontal plane, the total unit weight, and the small strain shear modulus $G_{max}$ for each soil layer. The latter was estimated from correlations between inferred $N_{1,60}$ values and $G_{max}$ for sand and gravel soils (Seed et al, 1984). No cyclic pore pressure generation was considered in the DESRA-2C model. The neglect of pore pressure generation will lead to a conservative prediction of shear stresses and accelerations transmitted.

Based on the inferred $N_{1,60}$ values computed from the Becker Density Test measurements, cyclic resistance ratios (CRR = cyclic shear strength divided by the vertical effective pressure) were computed using methods outlined by Idriss and Boulanger (2006) considering an effective magnitude 7 earthquake. The CRR values were then compared to the effective cyclic shear stress ratios (CSR) computed from the DESRA-2C analysis. This comparison indicated that liquefaction triggering was likely above the 8 m depth and possibly in thin lenses at larger depths in localized loose to compact sand or sand and gravel layers.

BC Hydro had specified that post-seismic movements of the raft slab were not to exceed 75 mm. Using empirical correlations between Standard Penetration Test $N_{1,60}$ values (inferred from previous BDT data) and CSR, estimates of post-seismic volumetric recompression of liquefied soils were made based on the method by Wu (2003). The calculations indicated post-seismic settlements of about 180mm considering that extensive liquefaction occurs between the 4 and 8m depth.

Peak shear strains on the horizontal plane computed from DESRA-2C indicated that even with the assumption of no excess pore pressure generation during shaking that high shear strain development could occur in the looser sand and gravel materials between 4 and 12 m depth. Peak strain values of 2% were computed.  The latter correspond to peak lateral displacements relative to the input base displacements of about 90 mm and permanent lateral displacements of about 55 mm based on integration of the strain time history values for each soil layer. Published data by Seed et al (2003) indicates that computed peak and residual lateral displacements would be significantly higher if pore pressure generation (and in the extreme liquefaction) occurs during shaking.  Shear strains in excess of 3% under level ground conditions were considered probable in the event of soil liquefaction.

Due to the presence of an unsaturated, non-liquefiable layer of sand, gravel and cobbles above the groundwater table at 4m depth, bearing capacity failure of the raft slab was not anticipated under design bearing pressures.  However, the potential magnitude of post-seismic settlements and lateral movements of the raft slab due to liquefaction between the 4 and 8m depth exceeds the displacement tolerances (75 mm) specified by BC Hydro for the structures. Therefore foundation improvement was specified as being required.

## Seismic Response Analysis of Jet Grout Columns

JG columns option was selected after a number of other different foundation improvement options were initially considered, including: 1) Demolition of the existing raft slab followed by vibro-replacement and reconstruction of the raft slab, 2) Demolition of the existing raft slab followed by sub-excavation to just above the water table and rapid impact compaction (RIC) below the excavation base and reconstruction of the raft slab and 3) Use of both vertical and battered micro-piles drilled through the existing raft slab to reduce post-seismic movements of the slab.

Four treated zones of jet grouting composed of four 1 m diameter tangent JG columns (jet grouted soil plus steel pipes having a 219mm OD and a 12.7 mm wall thickness) were proposed to provide foundation support at each corner of the raft slab which was to have a final dimension of 8.5 m wide x 14 m long x 1 m deep. The JG columns were to be constructed to a depth of 12.5m below the base of the raft slab, and each pipe pile was placed to a depth of 1m above the base of each column. The annulus between the steel pipe and the drill hole was specified to be filled using tremie placement methods with high strength Microsil grout having an unconfined compressive strength (UCS) of 35 MPa or greater. A summary of the computed structural properties of the JG columns and pipe piles based on an unconfined compressive strength of the JG column of 3 MPa and a yield stress of the steel pipe of 310 MPa is given in Table 1.

A two dimensional finite element model of the 1.0m thick raft slab incorporating two of the JG columns, each having an equivalent diameter of 2.0m, and half of the total mass of the slab was developed to examine the seismic response of the slab and JG columns. The computer program LSDYNA (Livermore Software, 2001) was used for the modeling. The superstructure (transformer) was represented as a "stick" model comprising a vertical beam 2.7 m above the top of the raft slab, supporting a lumped mass having a mass one-half of the superstructure.  Elastic-plastic beam elements were used to represent each JG column with the properties indicated in

Table 1. The JG column was assumed pinned (capable of transmitting shear, but zero moment transmission) at the underside of the raft slab. The soil profile and engineering properties of the various soil layers are identical to properties previously adopted for one dimensional site response analysis.

**Table 1 – Computed Structural Properties of the Jet Grouted Zone [1]**

| PROPERTY | VALUE | PROPERTY | VALUE |
|---|---|---|---|
| Equivalent Diameter (m) | 2.0 | Steel Pipe Shear Strength (MPa) | 176 |
| Soil-Grout UCS (MPa) | 3 | Steel Pipe Young's Modulus (MPa) | $2.08 \times 10^5$ |
| Soil-Grout Shear Strength (MPa) | 1.5 | Flexural Rigidity of JG Column + 4 Steel Pipes $(kN-m^2)$ | $6.47 \times 10^6$ |
| Soil-Grout Young's Modulus E (MPa) | $8.2 \times 10^3$ | Axial Rigidity of JG Column + 4 Steel Pipes (kN) | $3.26 \times 10^7$ |
| Steel Pipe Outside Diam. (mm) | 219 | Shear Capacity of JG Column + 4 Steel Pipes (MN) | 10.6 |
| Steel Pipe Wall Thickness (mm) | 12.7 | Yield Moment of JG Column + 4 Steel Pipes (MN-m) | 8.0 |
| Steel Pipe Yield Stress (MPa) | 310 | | |

Notes: (1) JG column assumed to consist of 4 contiguous 1m diameter columns, giving an overall effective diameter of 2.0m, with a steel pipe pile placed down the centre of each 1m diameter column.

Two phases of loading were applied to the FE model. The first phase consisted of a self-weight gravitational loading phase (including vertical loads applied to the footing) to develop effective stresses in each soil element and initial axial loads in the beam elements used to represent the JG columns. Drained soil properties were used for this phase of loading. The second phase of analysis, applied after the self-weight loading phase, consisted of applying horizontal seismic excitation to the (assumed) rigid base of the model with seismic inertial forces in each soil or beam element computed based on the total unit weights of the element. The input base motions were applied at 18 m depth based on accelerations computed from the earlier DESRA-2C analysis.

Undrained soil properties (zero volume change) were used during cyclic loading for soil elements below the water table that were considered liquefiable, i.e. those elements located between the 4 to 8 m and 10 to 12 m depths. Cyclic shear strengths and stiffness properties for the liquefiable soil layers were based on a total stress model without consideration of pore pressure generation during shaking. The properties of the cyclic stress-strain model were selected to limit the shear strength to the designated cyclic resistance ratio (CRR = limiting cyclic shear strength/vertical effective stress at the depth under consideration) for the soil layer. Soil properties were also calibrated to cause a target cumulative shear strain in single element tests subject to the limiting CRR value after 10 cycles of sinusoidal shear loading. The selection of 10 equivalent cycles of shaking corresponds approximately to consideration of a magnitude M7 design earthquake. The target cumulative shear strain was based on recommendations provided by Seed et al (2003), which is a function of the estimated corrected Standard Penetration Test $N1_{60}$ for the liquefiable soil layer being considered.

Soil and JG column interaction was represented using elastic-plastic lateral springs placed over the length of the column between the 2 and 11 m depth and spaced at 1 m depth intervals. Each JG column was assumed to exactly follow the near field soil motions in the compact to dense granular soils below 11 m depth, and therefore no lateral interaction springs were placed below this depth. The elastic-plastic characteristics of the lateral springs were selected using static "p-

y" curves computed using methods described by the American Petroleum Institute (2000) for granular soils.

The 2-D FE model (Model 1) was intended to compute lateral ground displacements and bending moments and shear forces within the JG columns to check structural design of the columns. However, the relatively stiff lateral springs used to represent interaction between the JG columns and the surrounding liquefiable soil mass resulted in the beam element nodes moving a similar amount to the adjacent near field soil node, and limiting the interaction forces (and hence the moments and shears along the column). This was not believed to be realistic and a separate beam column model (Model 2) describing the soil-column interaction was subsequently developed. Various runs of Model 1 indicated that use of the JG columns would be effective in reducing seismic lateral and vertical movements of the raft slab compared to the case where JG columns were not used to support the slab and that the level of seismic displacement of the slab would be within tolerances specified by BC Hydro.

Model 1 was used primarily to compute near field lateral ground displacements to be applied in Model 2. In Model 2, an individual JG column was represented using elastic-plastic beam elements (described previously), and added mass was applied at the top of the column to simulate the mass of the raft slab and transformer superstructure. Nonlinear springs were placed along the column at various depths to represent the near field interaction between the JG column and the adjacent soil. The time history of lateral ground displacements computed from Model 1 was then applied at the ends of the springs along the column. Since horizontal ground displacements relative to the input base motion were used, it was necessary to add in inertia forces corresponding to the mass of the beam elements times the input base acceleration. This comes from consideration of the differential equations of motion of the beam subject to time varying support excitation. The input base acceleration was the same as applied at the bottom of the 2-D finite element model.

Results of the Model 2 calculations indicated very similar amplitudes and frequencies of top of column lateral displacements as predicted using Model 1. To account for uncertainty in the magnitude of liquefaction induced, lateral ground displacement acting on the JG columns, the ground displacement amplitudes were tripled. This resulted in a maximum shear force and bending moment of 7.9 MN and 8.0 MN-m, respectively. These maxima occurred between the 7 and 8m depth, just above the base of the liquefiable layer. The computed maximum moment was at the estimated yield moment of the column, indicating that a plastic hinge formed near the base of the liquefied layer. The analyses demonstrated that shear failure of the proposed JG columns was unlikely since the maximum shear was less than the shear capacity of the section. Despite the plastic hinging, the column continued to carry the imposed weight of the superstructure and axial buckling did not occur. Permanent lateral and vertical displacements at the top of the column (underside of slab) at the end of shaking of 50mm and 42mm, respectively, were computed which are within the specified displacement tolerances of the raft slab (<75mm).

## Jet Grout Columns Construction and Quality Control

The various dynamic analyses carried out indicated that the shear and moment capacity of the JG columns should be adequate to withstand the anticipated lateral ground movements in the event

of soil liquefaction provided the JG columns were constructed as designed. Quality control utilizing a few different approaches and methods during construction was therefore essential.

Matcon Excavation and Shoring Ltd. carried out construction of the JG columns following a "performance type" specification using a double fluid (air and grout fluid) jet grouting method. Grout manufactured from Portland Type 10 cement was mixed with water to achieve a minimum target grout density of 1500 kg./cu.m. A special equipped drilling rig with a hollow rotary head was used. Special tooling (double rods, nozzles, grout mixer and pumps) created the grout jet need for the disaggregation and mixing of the soil. After drilling to the required depth, the jet is created, withdrawing the rods at constant speed and rotation and the soil is eroded and mixed. It is always good practice at the start of a JG project to carry out a field test with 3 or 4 columns and different jetting parameters. For this project, this was impossible due to the shortage of space within the substation and the contractor used his experience to select conservative parameters for column construction.

Drilling difficulties were periodically encountered in zones containing cobbles which slowed production rates.  Wood debris was also encountered at shallow depths.  At some depths, return of the injected grout to the ground surface ("reflow") was low due possibly to blockage within the annulus between the wall of the drillhole and the drill string. In these cases, the jetting was stopped since the reflow is essential to prevent undesirable over-pressures and the hole was cleaned out. Some reflow was lost at shallow depths under the slab in gravelly areas with high lateral permeability.

As part of the QA program the following methods were selected which are described in more details below: 1) Sampling and UCS testing, 2) Continuous coring and logging of the constructed JG columns, 3) Downhole Video Imaging (DVI) of the constructed JG columns, 4) Downhole Sonic Integrity Testing (SIT) of the constructed JG columns and 5) Estimating the effective radius of the constructed JG columns.

### UCS Testing of Grab and Core Samples

During JG column construction, grab samples of the grout-soil mix were obtained at the ground surface from the reflow. Depths of the grab samples were estimated from the known depths of the drill rods (3, 5, 7 & 9 m) at the time of sampling. The grab samples were used to make Unconfined Compressive Strength (UCS) cube samples for further strength testing at 7 day, 14 day and 28 day intervals.  UCS testing of 64 grab samples which were 28 days old indicated that 90% of samples gained UCS strengths greater than 3 MPa which was the target strength. Figure 3 shows plotted UCS strength values of the grab samples versus depth.

UCS measurements were also statistically analyzed to compute the mean – 1 standard deviation (SD) of the strength gain versus time as plotted in Figure 4.  The trend of the data is to show a progressive increase in strength with time.  The mean – 1 SD 28-day UCS values from grab samples are in excess of 3 MPa below about the 3m depth which is the depth range where highest seismic bending moments and shear forces occur in the JG columns.  Thus, the available UCS data indicate the required strengths of the JG columns from the seismic response analysis have been obtained.
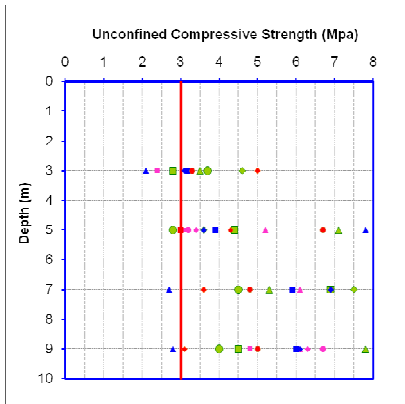
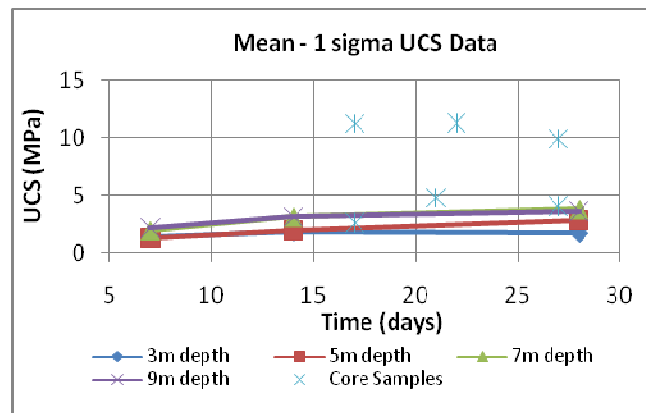Figure 3: UCS (28 day) strength of grab samples versus depth



Figure 4: Mean -1 SD UCS strength gain versus time.

The data were also compared against UCS measurements of 6 core samples obtained from the constructed JG columns. It should be noted that core samples were selected from intervals judged to be well cemented. The UCS data from the core samples are seen to cover the range indicated by the grab samples so that we consider the grab sample data to provide a reasonable and possibly conservative evaluation of in-situ column strengths.

Two of the 6 core samples obtained from the constructed JG columns were subjected to uniaxial compression test with stress-strain measurements. The peak strengths were achieved at relatively small axial strains (less than 0.5%) which are representative of brittle behavior.

We also compared the UCS values with cement content (ratio of dry weight of cement to dry weight of soil solids x 100%) as proposed by Haeri et al, (2006). The data gathered by Haeri et al (2006) are available only over a limited range of cement contents but have been extrapolated to a cement content of 20%. The latter has been previously estimated as broadly representative of the cement content within the JG columns constructed. This strength extrapolation indicates a 28-day UCS strength value of 5 MPa which is in good agreement with grab sample mean data.

## Coring of Jet Grout Columns

Continuous coring of 5 of the JG columns was also carried out at distance of ~300mm from the center of a column using rotary drilling procedures and a triple tube HQ3 core barrel (61 mm in diameter). Coring was carried out to 13 m below the top of slab and borehole logs were prepared documenting types of material recovered and lengths of recovered cores. It is always difficult to have a good core recovery in jet grouted columns in cobblely/gravelly soils and although at most intervals the integrity of cores was indicative of proper cementation/grouting, there were intervals where degree of cementation and integrity of cores did not seem to be satisfactory.

These intervals with lower degrees of cementation were above the 7.6m depth where previous Becker drilling indicated the highest cobble and coarse gravel content. Careful observation of the core samples indicated small bits of grout adhering to larger gravel or cobble particles and core

recovery was in the range of 0 to 20% along those intervals. At other locations, the larger particles were well bonded by the grout where the core recovery was 90 to 100%. There were initially some concerns that the coring was indicating less than acceptable degrees of grouting of the soil mass.  However, it was judged that the coring process could break out larger particles, which would subsequently be washed free of grout by the drilling fluid. Larger particles (gravel, cobbles) could also block the core barrel, preventing adequate recovery. Thus, the quality of grouting along these sections was further assessed using different methods (downhole video imaging and sonic integrity testing) which confirmed that the quality and integrity of the JG columns had been achieved.

## Downhole Video Imaging (DVI)

During the continuous coring process it was unclear as to whether the intervals with little core recovery were giving adequate pictures of the degree of cementation within the JG column due to the drilling process. A DVI survey was therefore conducted to obtain video images of the walls of the cored borehole cavities using a downhole video camera. DVI was undertaken at 4 of the constructed JG columns that were cored and flushed with clear water at the completion of coring.

The obtained video images showed clearly good mixing of the grout into the soil pores and a well bonded soil matrix.  These video images indicated that the cementation pattern at intervals where the core recovery was small (0 to 20% corresponding to the presence of gravel and cobbles) were very similar to those intervals whose core recovery was 90 to 100% (in pure sand locations). At some locations it could be seen that the drilling process had dislodged larger gravel or cobble particles from the adjacent grouted zones.  Thus, it was confirmed that the previous coring had caused disturbance to the grouted sand, gravel and cobbles and would not necessarily provide a true indication of the degree of cementation, especially in coarse gravel and cobble zones.
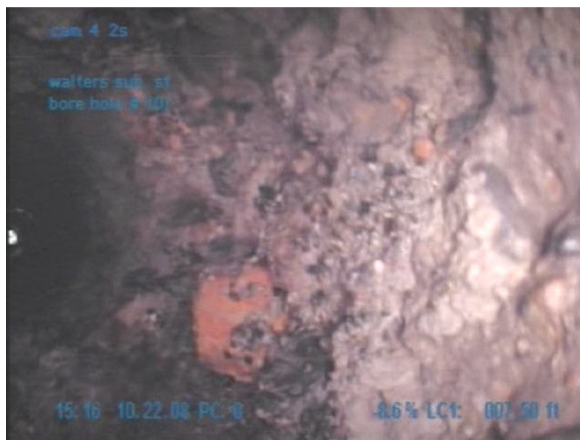


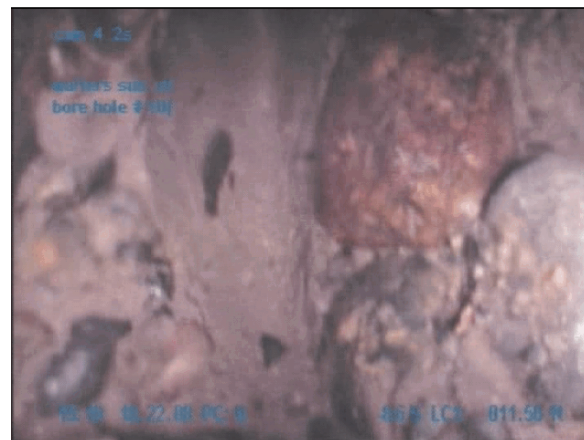Figure 5: DVI of a fine sand and gravel interval with high core recovery



Figure 6: DVI of a coarse gravel and cobble interval with low core recovery

## Sonic Integrity Testing (SIT)

Downhole Sonic Integrity Testing (SIT) at 3 columns was conducted to measure average compression wave velocities a minimum of 14 days after completion of jet grouting. The data were used to determine whether a reflected wave from the column base could be detected, as this is considered to provide a measure of column continuity and column stiffness. Measurements of acceleration versus time for each accelerometer showed average column compressive wave speeds at three of the JG columns were 1470, 2800 and 3600 m/s (or elastic shear wave velocities of about 700 to 1800 m/sec assuming an average Poisson's ratio of 0.3). These values are 10 times higher than elastic shear wave velocities (150 to 300 m/s) typically measured in unbonded sand and gravel subsoils at other sites in the area. The SIT results showed strong wave reflections from the bases of the columns and from this it was concluded that reasonably good cementation over the full length of the columns was obtained.

## Estimates of Jet Grout Column Diameter

Gross volumes of grout used to form each column were provided by Matcon. Net grout volumes were computed from the volumes of waste spoil that were removed using pumper trucks. The latter are considered to be approximate quantities since some of the reflow was lost in permeable upper zones (leading to too low a volume of waste) and the waste was also diluted from water additions during cleaning of the drill rods (leading to an over-estimate of waste volume). Despite these measurement limitations, an estimate of the effective diameter ($D_{eff}$) of grouting was obtained by calculating the volume of voids within a total volume ($\pi D_{eff}^2/4$)L where L is the total length of the column, based on an assumed average void ratio for the soil formation. Jet grouting fluidizes and mixes the soils and so it has been



Figure 7: Estimated column diameters
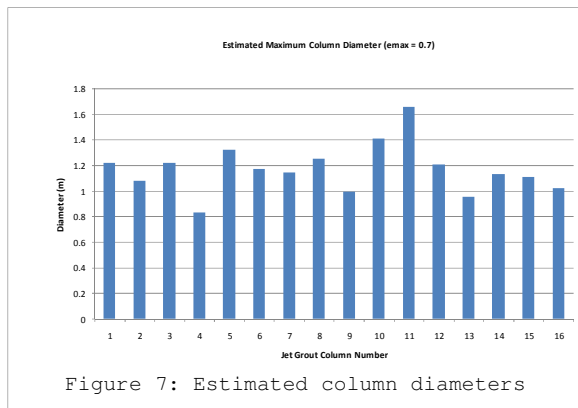
assumed that the void ratio of the predominantly sand and gravel soil mass will approach the maximum (loosest) void ratio (= $e_{max}$). Assuming an $e_{max}$ value of 0.7, typical of gravelly sand soils, the effective diameter of each JG column was calculated based on the net volume of grout injected into the voids, as shown in Figure 7. This indicated an average column diameter of 1.17m, satisfying the general intent of the specification. Further development of methods to accurately measure JG column diameters is clearly required by the industry. At the present time, in addition to column excavations (which were impractical for this site), the only feasible methods involve coring to map out the general zones of grouting, along with downhole video imaging.

## Conclusions

The use of dynamic soil-column interaction analysis was important to evaluate bending and shear demand of JG columns used to minimize seismic displacements of a raft slab where soil liquefaction effects were important. The analysis was used to design the diameter and strength characteristics of the columns. Upon overall review of the QA data, it was concluded that

continuous G columns were constructed properly with effective diameters $D_{eff}$ of at least 1m per column and having adequate strength properties. UCS testing of grab samples indicated that a reasonable minimum evaluation of in-situ column strengths can be obtained from the grab samples' strength values. The use of DVI was considered to be particularly useful in identifying in a continuous manner the degree of cementation along a column especially where the core recovery was poor. SIT also provided an adequate confirmation of the increase of the shear wave velocity of the treated mass.

## Acknowledgements

## List of References

American Petroleum Institute (2000), "Recommended Practice for Planning, Designing and Constructing Fixed Offshore Platforms, API Recommended Practice 2A-RP2A, 21Ed., Apr 2000

Haeri, S.M., et al (2006), "Effect of Cement Type on the Mechanical Behavior of Gravelly Sand", Geotechnical and Geological Engineering, vol. 24, pp 335-360

Idriss, I.M. and R.W. Boulanger (2006), "Semi-Empirical Procedures for Evaluating Liquefaction Potential During Earthquakes", Soil Dynamics and Earthquake Engineering, vol. 26, pp. 115-130

Lee, M.K. and W.D.L. Finn (1978), "DESRA-2C User's Manual", University of B.C., Faculty of Applied Science

Livermore Software Technology Corp. (2001), "LS-DYNA User's Manual, Version 970", Livermore, California

Seed, H.B. et al (1984), "Moduli and Damping Factors for Dynamic Analyses of Cohesionless Soils", University of California, Berkeley, UCB/EERC Report 84-14

Seed, R.B. et al (2003), "Recent Advances in Soil Liquefaction Engineering: A Unified and Consistent Framework", 26th Annual ASCE Los Angles Geotechnical Spring Seminar, H.M.S. Queen Mary, Long Beach, Calif., April 30, 2003

Sy, A. (1997), "Twentieth Canadian Geotechnical Colloquium: Recent Developments in the Becker Penetration Test: 1986-1996", Canadian Geotechnical Journal, vol. 34, pp. 952-973

Wu, J. (2003), "Liquefaction Triggering and Post Liquefaction Deformations of Monterey 0/30 Sand Under Uni-Directional Cyclic Simple Shear Loading", Ph.D. dissertation, University of California, Berkeley